Alzheimer's & Dementia: Diagnosis, Assessment & Disease Monitoring 10 (2018) 253-259

Special Section: State of the Field: Advances in Neuroimaging from the 2017 Alzheimer's Imaging Consortium

Similar pattern of atrophy in early- and late-onset Alzheimer's disease

Carl Eckerström[a,*], Niklas Klasson[a], Erik Olsson[a], Per Selnes[b,c], Sindre Rolstad[a], Anders Wallin[a]

[a]Institute of Neuroscience and Physiology, University of Gothenburg, Gothenberg, Sweden
[b]Department of Neurology, Akershus University Hospital, Lørenskog, Norway
[c]Institute of Clinical Medicine, Campus Ahus, University of Oslo, Oslo, Norway

Abstract

Introduction: Previous research on structural changes in early-onset Alzheimer's disease (EOAD) and late-onset Alzheimer's disease (LOAD) have reported inconsistent findings.
Methods: In the present substudy of the Gothenburg MCI study, 1.5 T scans were used to estimate lobar and hippocampal volumes using FreeSurfer. Study participants (N = 145) included 63 patients with AD, (24 patients with EOAD [aged ≤65 years], 39 patients with LOAD [aged >65 years]), 25 healthy controls aged ≤65 years, and 57 healthy controls aged >65 years.
Results: Hippocampal atrophy is the most prominent feature of both EOAD and LOAD compared with controls. Direct comparison between EOAD and LOAD showed that the differences between the groups did not remain after correcting for age.
Discussion: Structurally, EOAD and LOAD does not seem to be different nosological entities. The difference in brain volumes between the groups compared with controls is likely due to age-related atrophy.

Keywords: Early-onset AD; Late-onset AD; MRI; Neuroimaging; Hippocampus

1. Introduction

Alzheimer's disease (AD) is the most common type of dementia and is believed to account for approximately 50 to 70% of all cases of dementia [1]. AD is characterized by typical neuropathological changes, neurofibrillary tangles, and senile plaques, gradually spreading throughout the brain [2]. Traditionally, AD is categorized as either early-onset Alzheimer's disease (EOAD, age ≤65 years) or late-onset Alzheimer's disease (LOAD, age >65 years). EOAD is thought to have a faster rate of progression and shows a greater neuropathological burden than LOAD [3]. Cognitively, LOAD is characterized by a classic AD profile with impaired semantic memory function as the most prominent finding whereas EOAD may present a more atypical profile with apraxia and impaired visuospatial functions [4]. Structural imaging studies have been performed to elucidate whether EOAD is AD with an earlier starting point or if EOAD should be regarded as a different nosological entity. The interpretation of these imaging studies is complicated by generally small group sizes and different methodological approaches. Although not consistent, most studies have reported a higher degree of neocortical atrophy in EOAD compared with LOAD [5–9]. Although some studies do not find a difference in hippocampal atrophy between EOAD and LOAD [9,10], most studies report more pronounced hippocampal atrophy in LOAD [5,6,8,11].

A better understanding of the structural brain changes taking place in AD and their relation to age at onset would be useful to improve inclusion criteria in future intervention studies and also for increasing the etiological/nosological understanding of the disease. Furthermore, as patients with dementia diseases often undergo an incipient phase when

The authors have no competing interests to report.
*Corresponding author. Tel.: +46 31 3438668; Fax: +46 31 7769055.
E-mail address: carl.eckerstrom@neuro.gu.se

https://doi.org/10.1016/j.dadm.2018.02.001

differential diagnostics can be difficult, information on patterns of atrophy in AD at different ages of onset will be highly valuable.

The aim of the present study is to investigate if EOAD and LOAD have different patterns of atrophy compared with healthy controls of similar age and also by direct comparison between EOAD and LOAD.

2. Materials

2.1. The Gothenburg MCI study

The Gothenburg MCI study is a clinically based longitudinal study that aims at identifying neurodegenerative, vascular, and stress-related disorders before the development of dementia [12]. The Gothenburg MCI study is approved by the Local Ethics Committee (diary number: L091-99, 1999; T479-11, 2011). Inclusion requires subjective and/or objective (by an informant) verifications of a progressive cognitive impairment for more than 6 months, age $\geq$50 and $\leq$ 79 years, and Mini–Mental State Examination (MMSE) score $\geq$18. Exclusion criteria are acute/instable somatic disease, severe psychiatric disorder, or substance abuse.

Healthy controls were recruited from senior citizens' organizations. Controls were not included if they had subjective or objective signs of cognitive disorder as assessed with the aforementioned procedure or fulfilled any of the aforementioned exclusion criteria.

2.2. Classification

Patients' degree of decline was staged according to the Global Deterioration Scale (GDS). GDS classification is made by means of checklists and instruments for cognitive symptoms [12]. The guidelines for the classification used are as follows: for GDS 4 (mild dementia) participants should have MMSE $\leq$ 25, clinical dementia rating sum of boxes $>$ 1.0, investigation of flexibility $>$ 3, and two or more positive outcomes on variables 13 to 20 of stepwise comparative status analysis [13]. When the guidelines are not applicable, a consensus decision among physicians at the clinic is made to determine appropriate GDS score. All patients classified as GDS 4 were further assessed by a specially trained physician for specific dementia diagnosis. Anamnestic and clinical symptomatology and the presence of cerebral white matter changes determined by a modified version of the Fazekas scale were taken into account in the diagnostic procedure [14]. If the diagnosis cannot be unambiguously determined, then it is further discussed and established in a clinical consensus meeting. AD is diagnosed using the NINCDS-ADRDA criteria for AD [15]. For an AD diagnosis, the patient must have at most only mild white matter changes and predominant temporoparietal lobe symptoms. This was done to ensure that no patients with mixed dementia were classified as AD. Only patients with GDS 4 and an AD diagnosis were included in the present study. The guidelines and diagnostics are described in detail in a previous publication [12].

2.3. The present study

The present study is a substudy of the Gothenburg MCI study. An additional inclusion criterion for all participants was a magnetic resonance imaging scan using a Siemens Symphony 1.5 T scanner available for analysis. Patients also had to be classified as GDS 4 and subsequently received an AD diagnosis according to the NINCDS-ADRDA criteria.

The total patient group (N = 145) consisted of 63 patients with AD and 94 healthy controls. Of the 63 AD patients, 24 were $\leq$65 years and classified as EOAD, and 39 were $>$65 years, that is, LOAD. Of the healthy controls, 25 were $\leq$65 years, and 57 were $>$65 years. Patients with mixed dementia or vascular dementia were not included in the study.

3. Methods

A 1.5 T scanner (Siemens Symphony, Erlangen, Germany) was used for the magnetic resonance data acquisition. FreeSurfer volumetry was performed on T1 3D inversion recovery/gradient recalled images (repetition time 1610 ms, echo time 2.38 ms, flip angle 15°, coronal slices, field of view 250 mm $\times$ 203 mm, slice thickness 1 mm, pixel spacing 0.49 mm $\times$ 0.49 mm, and matrix size 512 $\times$ 416).

Cerebrospinal fluid (CSF) samples were collected by lumbar puncture. CSF T-tau and amyloid β 42 levels were determined using a sandwich enzyme-linked immunosorbent assay constructed to measure T-tau or amyloid β 42 [16].

3.1. FreeSurfer

Brain volumes were measured using the automated segmentation software, FreeSurfer, version 5.3.0, which is freely available for download online [17]. The FreeSurfer analyses were performed on a computing cluster running 64 bit CentOS 6. These analyses were performed on nodes based on Supermicro X9DRT Intel E5-2670 (Sandy Bridge) running at 2.6 GHz. A few analyses were also performed using a MacPro 3.1 with 64 bit 2 GHz $\times$ 2.8 GHz quad-core Intel Xeon processors and Mac OSX 10.8.5.

The calculation of surface volumes in FreeSurfer begins with an affine alignment to the MNI305 atlas, an intensity normalization, and removal of the skull [18,19]. Voxels are then classified as white matter or nonwhite matter by a threshold classification that is refined by some assumptions of the classification of the given voxel and its neighboring voxels [18]. Seed points in corpus callosum and the pons from the atlas alignment are then used to find two cut planes to separate the hemispheres and to remove subcortical structures [18]. A white matter surface is then generated for each hemisphere by the outer boundary of the white matter volume and some refinement based on intensities gradients [18,20]. The pial surface is then deformed outward from the white matter surface trying to find the largest shift in

intensities that would indicate the border between gray matter and CSF [18,20]. A topology correction is performed [21,22] and then a parcelation of the cortex (defined by the surfaces) by the use of an atlas [23].

The calculation of subcortical volumes also begins with some preprocessing including an affine alignment to the MNI305 atlas, intensity normalization, and removal of the skull [19,24,25]. Then the segmentation proceeds using a probabilistic atlas. The probabilistic atlas contains three types of probability estimates based on data from a number of manually segmented scans: (1) a Gaussian model of the intensity distribution of each tissue class; (2) the relative frequency of occurrence at each atlas location for each tissue class; and (3) the relative frequency of occurrence at each neighboring atlas location for each tissue class given a specific atlas location and a specific tissue class. Using these probabilities, an initial segmentation is generated, and an iterated conditional modes algorithm is executed to assign each image voxel a correct tissue class. The iterative process proceeds until no voxel changes occur in terms of tissue classification [24].

Once the process had finished, subcortical volumes were extracted using the aparcstats2table script, and lobular volumes constructed according to the instructions on the FreeSurfer homepage [26].

A two-step approach was used for quality control of the FreeSurfer output using the FreeSurfer graphical user interface Freeview (https://surfer.nmr.mgh.harvard.edu/fswiki/FreeviewGuide/FreeviewIntroduction). First, all volumes were inspected by author N.K. No or minor errors were accepted. The remaining volumes were flagged. Second, all flagged volumes were inspected by author C.E. who excluded all regions containing meaningful errors (approximately >10% of the volume). Typical errors were the exclusion of brain matter in anterior parts of the temporal lobes and inferior parts of the frontal lobes. Both raters were blinded to group belonging and other patient data. Only a few patients had more than one region excluded from the analyses.

The following data were excluded: 10 frontal lobes (5 AD patients [2 EOAD and 3 LOAD], 5 controls), 1 parietal lobes (1 control), 36 temporal lobes (15 AD patients [8 EOAD and 7 LOAD], 21 controls), and 3 occipital lobes (controls).

All FreeSurfer volumes were normalized using FreeSurfer's estimate of intracranial volume (eTIV). The residual normalization method has been described in a previous publication [27]. Briefly, a regression analysis was performed in the control group to obtain a regression coefficient (k), reflecting the association between eTIV and the region of interest which was then applied to the test group according to the formula: $V_{norm} = V_{abs} - k*(eTIV - Mean[eTIV])$.

3.2. Statistical analyses

Demographics and differences were analyzed with the unpaired *t*-test (age, MMSE, and education) and χ^2 (sex). Group differences in CSF markers were analyzed with the unpaired *t*-test. Group differences in brain volumes were evaluated using analysis of covariance with age as a covariate. To assess the diagnostic value of the imaging variables, group comparisons were then repeated for younger participants (age ≤65 years), older participants (age >65 years) using receiver operating characteristic and binary logistic regression with "EOAD" or "LOAD" as dependent variable and one of the imaging variables as independent variable. Finally, a direct group comparison between EOAD and LOAD was performed using binary logistic regression with EOAD as dependent variable, analysis of covariance with age as a covariate, and a *t*-test where the volumes have been corrected for the influence of age using the same method as for the normalization for intracranial volume (*t*-test [corrected]). All analyses were performed using SPSS (version 19.0).

4. Results

EOAD has lower MMSE scores and more pathological values on CSF markers compared with controls (Table 1). Furthermore, EOAD has smaller hippocampi, cingulate gyri, and frontal lobes compared with age matched controls. When comparing the older study participants, all measured brain volumes are smaller in LOAD.

4.1. EOAD compared with younger controls

The same markers (left/right hippocampus, cingulate gyri, and frontal lobes) that were significant in the group comparison provided the best predictive values as can be

Table 1
Demographics and volumetric data for study participants separated by age (≤/> 65 years)

	Age ≤65 years		Age >65 years	
Variable	EOAD	Controls	LOAD	Controls
N	24	25	39	57
Age	61.2 ± 3.1	60.7 ± 2.9	72.3 ± 4.9	70.6 ± 4.7
Females (%)	55	55	56	67
MMSE	21.8 ± 5.4**	29.2 ± 1.7	22.1 ± 4.5**	29.3 ± 0.9
Education, years	11.0 ± 2.8*	13.9 ± 3.5	11.6 ± 3.6	12.8 ± 3.6
T-tau (ng/L)	612 ± 293**	261 ± 160	667 ± 301**	308 ± 122
Aβ42 (ng/L)	367 ± 205**	684 ± 252	368 ± 137**	646 ± 262
Left HC	3.0 ± 0.7**	3.9 ± 0.4	2.7 ± 0.6**	3.6 ± 0.6
Right HC	3.1 ± 0.6**	4.0 ± 0.4	2.7 ± 0.6**	3.6 ± 0.7
Cingulate gyri	18.4 ± 2.0*	19.9 ± 1.6	17.9 ± 2.6*	19.4 ± 2.2
Frontal	102.6 ± 7.9**	112.3 ± 8.4	99.3 ± 16*	107.8 ± 9
Parietal	82.9 ± 8.0	83.6 ± 7.4	78.5 ± 16.1*	83.0 ± 6.4
Temporal	94.8 ± 10.2	96.3 ± 12.7	93.0 ± 19.3*	96.7 ± 8.7
Occipital	42.2 ± 4.2	44.4 ± 4.4	40.0 ± 8.2*	43.8 ± 4.0

Abbreviations: EOAD, early-onset AD; LOAD, late-onset AD; HC, hippocampus; MMSE, Mini–Mental State Examination; Aβ42, amyloid β 42.

NOTE. Age, education years, MMSE scores, and volumetric data (cm^3) are presented as mean value ± SD.

*P value < .05 versus Controls, **P value < .001 versus Controls.

seen in Table 2. The receiver operating characteristic and regression analyses indicate that hippocampal volumes are the best markers with right hippocampus slightly outperforming left hippocampus.

4.2. LOAD compared with older controls

Results from analyses comparing LOAD with older controls are displayed in Table 3. Both the receiver operating characteristic analysis and regression analysis give high values for hippocampal volume in the differentiation between the groups. Left and right hippocampal volume stands out as excellent markers compared with the other volumetric markers.

4.3. Direct comparison between EOAD and LOAD

As displayed in Table 4, the group comparisons correcting for age show no significant differences between the groups (analysis of covariance, *t*-test [corrected]). Despite the fact that grouping was based on age, the logistic regression analysis indicate that only hippocampal volumes differed between the groups with, at best, moderate discriminative ability.

The scatter plots in Fig. 1 display the association between total hippocampal volume and age in the AD group and control group separately. The left pane shows a clear decrease in hippocampal volume with increasing age but no clear increasing or decreasing divergence between the groups as an effect of age. The right pane shows hippocampal volumes after correcting for the effect of age. Again, no clear divergence between the groups in different ages can be seen.

5. Discussion

The present study investigated hippocampal volume and cortical lobar volume in patients with AD and healthy elderly controls divided by age into younger/older groups. The main finding is that both EOAD and LOAD are characterized by smaller hippocampal volumes compared with the control groups. In addition, after correcting for age-related atrophy, no significant group differences remained between EOAD and LOAD.

Table 2
Comparison between EOAD and younger controls

	ROC	Binary logistic regression		
Region	AUC	Wald	*P* value	Correct classification %
Left HC	.87	13.1	<.001	80
Right HC	.89	13.7	<.001	82
Cingulate gyri	.72	6.5	.011	59
Frontal lobes	.79	9.6	.002	70
Parietal lobes	.51	0.1	.76	53
Temporal lobes	.54	0.1	.71	54
Occipital lobes	.66	2.8	.09	58

Abbreviations: ROC, receiver operating characteristic; AUC, area under the curve; EOAD, early-onset AD; HC, hippocampus.

Table 3
Comparison between LOAD and older controls

	ROC	Binary logistic regression		
Region	AUC	Wald	*P* value	Correct classification %
Left HC	.91	23.0	<.001	84
Right HC	.89	22.3	<.001	84
Cingulate gyri	.67	7.5	.006	63
Frontal lobes	.71	7.9	.005	70
Parietal lobes	.54	3.2	.08	66
Temporal lobes	.51	1.2	.28	60
Occipital lobes	.65	6.5	.01	67

Abbreviations: ROC, receiver operating characteristic; AUC, area under the curve; LOAD, late-onset AD; HC, hippocampus.

The patterns of atrophy in the EOAD and LOAD groups are quite similar. Compared with controls, both EOAD and LOAD have smaller hippocampi as the most prominent feature. In addition, LOAD has smaller volumes in all measured cortical lobar volumes in contrast to the EOAD group which only differed concerning cingulate gyri and frontal lobes. Although significantly smaller, the cortical structures had markedly lower predictive power compared with hippocampal volume. Previous studies have found hippocampal atrophy as the most prominent feature in LOAD [5–8,10,11,28–30], but the findings differ regarding atrophy in EOAD. Most studies have found hippocampal atrophy also in EOAD but only a few share our finding of hippocampal atrophy as the prominent marker [29,30], whereas others have found hippocampal atrophy in addition to atrophy of the cingulate [6,9,28], frontal [6], temporoparietal [7–9,28,31], and occipital [7,8] areas. As findings pertaining to EOAD are clearly diverging between studies, it is difficult to arrive at a conclusion. The proposed mechanisms for the studies finding widespread cortical atrophy in EOAD is that EOAD is different to LOAD in both neuropathological distribution and etiology, where EOAD is more attributed to genetic factors and

Table 4
Direct comparison between EOAD and LOAD

	Binary logistical regression			ANCOVA	*t*-test (corrected)
Region	Wald	Sig.	Correct classification %	*P* value	*P* value
Left HC	3.7	.05	68	.73	.80
Right HC	6.2	.01	64	.80	.54
Cingulate gyri	0.5	.47	62	.84	.37
Frontal lobes	0.8	.38	60	.62	.27
Parietal lobes	1.5	.22	63	.12	.23
Temporal lobes	0.1	.73	67	.72	.62
Occipital lobes	1.4	.24	57	.61	.28

Abbreviations: LOAD, late-onset AD; EOAD, early-onset AD; ANCOVA, analysis of covariance; HC, hippocampus.

NOTE. ANCOVA was performed with age as a covariate. *t*-test (corrected) was performed after correcting for the influence of age as detailed in the statistics section.

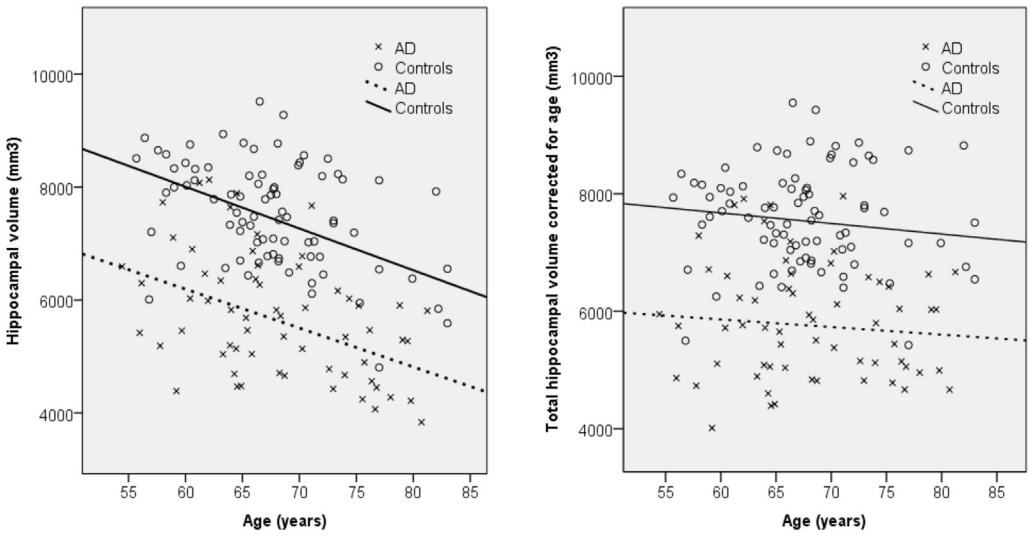

Fig. 1. Scatter plot for total hippocampal volume versus age for AD patients and control subjects. Left panel: Uncorrected model. AD: R^2 linear = 0.154. Control subjects: R^2 linear = 0.154. Right panel: Hippocampal volumes corrected for age. AD: R^2 linear = 0.006. Control subjects: R^2 linear = 0.011. Abbreviation: AD, Alzheimer's disease.

LOAD more environmental factors. The greater clinical variability of the EOAD group has led to the identification of nonamnestic subgroups with different clinical presentation and likely different underlying patterns of atrophy [4,32]. Therefore, a possible explanation for the diverging results could be the composition of the EOAD group. Ossenkoppele et al. [29] have evaluated the early stages of three subtypes of AD, finding that while amnestic EOAD had atrophy of the hippocampal-posterior cingulate circuit, the language- and visual-variants had atrophy of these underlying circuits. These findings highlight the importance of a stringent classification of the AD group, and especially so for the EOAD group. Although we have not performed a subgroup classification of AD patients in the Gothenburg MCI study, the diagnostic algorithm in use relies on cognitive profiles, where patients with AD should exhibit a primarily temporoparietal symptom profile. A consequence of our diagnostic procedure may be that we have a proportionally higher level of amnestic EOAD patients compared with previous studies. A high level of amnestic EOAD patient could explain our findings of hippocampal atrophy as the prominent feature in EOAD as well as LOAD. In addition, our approach to strict exclusion of patients with more than minor white matter lesions from the AD group might have affected the results compared with previous studies and possibly explain why we did not find more hippocampal atrophy in LOAD than in EOAD after correcting for age.

The hippocampal region is known to be one of the brain regions most affected by aging [33]. Direct comparisons between EOAD and LOAD show that hippocampal volume is the only marker that differs between the groups, but the difference disappears when correcting for age. It can therefore be concluded that a large part of the difference is due to age-related atrophy. The degree of atrophy is slightly higher in the LOAD group (19% in EOAD, 25% in LOAD compared with controls), but Fig. 1 suggests that while controls have smaller hippocampi when they are older, the gap between controls and AD patients remain intact. It has been shown that the rate of hippocampal atrophy in healthy aging accelerates with increasing age [33,34], which suggest that the smaller hippocampi in the LOAD group could be due to accelerated age-related atrophy. Although these findings should be interpreted with caution, they could be underlying the suggestion of more pronounced involvement of the hippocampi in LOAD. This would partly support a hypothesis about different regional vulnerability in EOAD and LOAD regarding hippocampal vulnerability in LOAD but fail to support the part on cortical vulnerability in EOAD [6]. However, if age-related and neurodegenerative changes provide a synergistic detrimental effect on the hippocampus, it could explain why the EOAD group have comparatively less atrophy and still a similar symptom profile.

5.1. Limitations

Although the group sizes were of a similar size as of most previous studies, they were still small, and the findings should be replicated in larger studies. In addition, we lack data on subtypes of AD as outlined previously. The EOAD and LOAD groups exhibit a similar cognitive function as measured with the MMSE and similar levels of CSF markers, but the distribution of AD subtypes may nonetheless be different between the groups, possibly affecting the results. Finally, we had some problems with the segmentation procedure where some data were lost in the quality control. This problem was most pronounced in the temporal lobes, resulting in the loss of 1/3 of all temporal lobes in the EOAD group and 18% of temporal lobes in the LOAD

group. The findings regarding the temporal lobes should therefore be interpreted with caution.

6. Conclusions

EOAD and LOAD exhibit a similar pattern of atrophy with smaller hippocampal volumes as the most pronounced difference compared with healthy controls.

Acknowledgments

This work was supported by grants from the Swedish Research Council (grants # 2002-5462, K2002-21P-14359-01A, and 09946), The Sahlgrenska University Funds, The Royal Swedish Academy of Sciences and Stiftelsen Psykiatriska Forskningsfonden. The funding sources were not involved in the drafting of this manuscript.

RESEARCH IN CONTEXT

1. Systematic review: We searched PubMed using the term "Early onset AD", "Early onset AD MRI", and "Early onset AD neuroimaging". Previous research on early-onset Alzheimer's disease (EOAD) has found that compared with late-onset Alzheimer's disease (LOAD), EOAD has comparatively more cortical atrophy whereas LOAD is characterized by mainly hippocampal atrophy. These findings suggest that EOAD is nosologically different from LOAD.
2. Interpretation: Our findings do not support the hypothesis that EOAD and LOAD are nosologically different. Previous finding might be explained by inclusion of patients with atypical Alzheimer's disease and inclusion of patients with concomitant pathologies such as white matter lesions.
3. Future directions: To fully address the question of the nosological status of EOAD, future studies need to: (1) provide a thorough classification of the patient group including phenotypic presentation, cognitive profile, and concomitant diseases; and (2) provide longitudinal investigations of the brain over a long time period.

References

[1] Qiu C, De Ronchi D, Fratiglioni L. The epidemiology of the dementias: an update. Curr Opin Psychiatry 2007;20:380–5.
[2] Braak H, Braak E. Neuropathological stageing of Alzheimer-related changes. Acta Neuropathol 1991;82:239–59.
[3] Marshall GA, Fairbanks LA, Tekin S, Vinters HV, Cummings JL. Early-onset Alzheimer's disease is associated with greater pathologic burden. J Geriatr Psychiatry Neurol 2007;20:29–33.
[4] Koedam EL, Lauffer V, van der Vlies AE, van der Flier WM, Scheltens P, Pijnenburg YA. Early-versus late-onset Alzheimer's disease: more than age alone. J Alzheimers Dis 2010;19:1401–8.
[5] Hamelin L, Bertoux M, Bottlaender M, Corne H, Lagarde J, Hahn V, et al. Sulcal morphology as a new imaging marker for the diagnosis of early onset Alzheimer's disease. Neurobiol Aging 2015; 36:2932–9.
[6] Moller C, Vrenken H, Jiskoot L, Versteeg A, Barkhof F, Scheltens P, et al. Different patterns of gray matter atrophy in early- and late-onset Alzheimer's disease. Neurobiol Aging 2013;34:2014–22.
[7] Migliaccio R, Agosta F, Possin KL, Canu E, Filippi M, Rabinovici GD, et al. Mapping the progression of atrophy in early- and late-onset Alzheimer's disease. J Alzheimers Dis 2015;46:351–64.
[8] Frisoni GB, Pievani M, Testa C, Sabattoli F, Bresciani L, Bonetti M, et al. The topography of grey matter involvement in early and late onset Alzheimer's disease. Brain 2007;130:720–30.
[9] Ishii K, Kawachi T, Sasaki H, Kono AK, Fukuda T, Kojima Y, et al. Voxel-based morphometric comparison between early- and late-onset mild Alzheimer's disease and assessment of diagnostic performance of z score images. AJNR Am J Neuroradiol 2005; 26:333–40.
[10] Cho H, Seo SW, Kim JH, Kim C, Ye BS, Kim GH, et al. Changes in subcortical structures in early- versus late-onset Alzheimer's disease. Neurobiol Aging 2013;34:1740–7.
[11] Cavedo E, Pievani M, Boccardi M, Galluzzi S, Bocchetta M, Bonetti M, et al. Medial temporal atrophy in early and late-onset Alzheimer's disease. Neurobiol Aging 2014;35:2004–12.
[12] Wallin A, Nordlund A, Jonsson M, Lind K, Edman A, Gothlin M, et al. The Gothenburg MCI study: design and distribution of Alzheimer's disease and subcortical vascular disease diagnoses from baseline to 6-year follow-up. J Cereb Blood Flow Metab 2016; 36:114–31.
[13] Wallin A, Edman A, Blennow K, Gottfries CG, Karlsson I, Regland B, et al. Stepwise comparative status analysis (STEP): a tool for identification of regional brain syndromes in dementia. J Geriatr Psychiatry Neurol 1996;9:185–99.
[14] Wahlund LO, Barkhof F, Fazekas F, Bronge L, Augustin M, Sjogren M, et al. A new rating scale for age-related white matter changes applicable to MRI and CT. Stroke 2001;32:1318–22.
[15] McKhann G, Drachman D, Folstein M, Katzman R, Price D, Stadlan EM. Clinical diagnosis of Alzheimer's disease: report of the NINCDS-ADRDA Work Group under the auspices of Department of Health and Human Services Task Force on Alzheimer's Disease. Neurology 1984;34:939–44.
[16] Andreasen N, Hesse C, Davidsson P, Minthon L, Wallin A, Winblad B, et al. Cerebrospinal fluid beta-amyloid(1-42) in Alzheimer disease: differences between early- and late-onset Alzheimer disease and stability during the course of disease. Arch Neurol 1999;56:673–80.
[17] FreeSurfer website. Home page. Available at: https://surfer.nmr.mgh.harvard.edu/. Accessed March 9, 2018.
[18] Dale AM, Fischl B, Sereno MI. Cortical surface-based analysis. I. Segmentation and surface reconstruction. Neuroimage 1999;9:179–94.
[19] FreeSurfer website. Pipeline Overview. 2015. Available at: http://surfer.nmr.mgh.harvard.edu/fswiki/FreeSurferAnalysisPipelineOverview. Accessed March 9, 2018.
[20] Fischl B, Dale AM. Measuring the thickness of the human cerebral cortex from magnetic resonance images. Proc Natl Acad Sci U S A 2000;97:11050–5.
[21] Fischl B, Liu A, Dale AM. Automated manifold surgery: constructing geometrically accurate and topologically correct models of the human cerebral cortex. IEEE Trans Med Imaging 2001;20:70–80.
[22] Segonne F, Pacheco J, Fischl B. Geometrically accurate topology-correction of cortical surfaces using nonseparating loops. IEEE Trans Med Imaging 2007;26:518–29.

[23] Fischl B, van der Kouwe A, Destrieux C, Halgren E, Segonne F, Salat DH, et al. Automatically parcellating the human cerebral cortex. Cereb Cortex 2004;14:11–22.
[24] Fischl B, Salat DH, Busa E, Albert M, Dieterich M, Haselgrove C, et al. Whole brain segmentation: automated labeling of neuroanatomical structures in the human brain. Neuron 2002;33:341–55.
[25] FreeSurfer website. ReconAllDevTable. 2015. Available at: https://surfer.nmr.mgh.harvard.edu/fswiki/ReconAllDevTable. Accessed March 9, 2018.
[26] FreeSurfer website. Cortical Parcellation. 2016. Available at: https://surfer.nmr.mgh.harvard.edu/fswiki/CorticalParcellation. Accessed March 9, 2018.
[27] Eckerstrom C, Olsson E, Borga M, Ekholm S, Ribbelin S, Rolstad S, et al. Small baseline volume of left hippocampus is associated with subsequent conversion of MCI into dementia: the Goteborg MCI study. J Neurol Sci 2008;272:48–59.
[28] Shiino A, Watanabe T, Kitagawa T, Kotani E, Takahashi J, Morikawa S, et al. Different atrophic patterns in early- and late-onset Alzheimer's disease and evaluation of clinical utility of a method of regional z-score analysis using voxel-based morphometry. Dement Geriatr Cogn Disord 2008;26:175–86.
[29] Ossenkoppele R, Cohn-Sheehy BI, La Joie R, Vogel JW, Moller C, Lehmann M, et al. Atrophy patterns in early clinical stages across distinct phenotypes of Alzheimer's disease. Hum Brain Mapp 2015;36:4421–37.
[30] van de Pol LA, Hensel A, Barkhof F, Gertz HJ, Scheltens P, van der Flier WM. Hippocampal atrophy in Alzheimer disease: age matters. Neurology 2006;66:236–8.
[31] Aziz AL, Giusiano B, Joubert S, Duprat L, Didic M, Gueriot C, et al. Difference in imaging biomarkers of neurodegeneration between early and late-onset amnestic Alzheimer's disease. Neurobiol Aging 2017;54:22–30.
[32] Mendez MF, Lee AS, Joshi A, Shapira JS. Nonamnestic presentations of early-onset Alzheimer's disease. Am J Alzheimers Dis Other Demen 2012;27:413–20.
[33] Fjell AM, McEvoy L, Holland D, Dale AM, Walhovd KB, Alzheimer's Disease Neuroimaging Initiative. What is normal in normal aging? Effects of aging, amyloid and Alzheimer's disease on the cerebral cortex and the hippocampus. Prog Neurobiol 2014;117:20–40.
[34] Crivello F, Tzourio-Mazoyer N, Tzourio C, Mazoyer B. Longitudinal assessment of global and regional rate of grey matter atrophy in 1,172 healthy older adults: modulation by sex and age. PLoS One 2014;9:e114478.